Efficiency and heat transport processes of low-temperature aquifer thermal energy storage systems: new insights from global sensitivity analyses

Authors: Luka Tas *, Niels Hartog, Martin Bloemendal, David Simpson, Tanguy Robert, Robin Thibaut, Le Zhang, Thomas Hermans

* corresponding author: luka.tas@ugent.be - Laboratory for Applied Geology and Hydrogeology, Department Geology, Ghent University, Belgium

Supplementary materials – Geothermal Energy

S1: Grid discretization and boundary conditions

The models of both cases cover an area of 1 km by 1 km around the ATES wells. For the ATES system, one warm well and one cold well are considered oriented perpendicular to the direction of the regional groundwater flow. The model of the thick productive aquifer ranges from the ground surface to the bottom of the Berchem and/or Voort aquifer. The model of the alluvial aquifer ranges from the ground surface to +35 mTAW allowing it to represent the thermal energy that may be lost to the layers below the production aquifer.

The ambient groundwater flow is modelled by setting a constant head (CHD) boundary in the north and south of the model and a no flux boundary for the east and west boundaries. On top of the model of the alluvial aquifer, recharge (specified flux boundary condition) was imposed. For the rest of the boundaries, the default option applies. For heat transport, all boundaries were set to the natural average temperature of the aquifer except for the top boundary of the alluvial aquifer which represents the soil temperature (details in 3.1). To model the injection and extraction of the ATES wells a specified flux as well as an injection temperature was imposed. The flow rate was distributed over the aquifer layers according to the transmissivity.

For hydrogeological models, the continuous model domain is discretized into a finite number of cells, within each of which difference equations are used to approximate the partial derivatives. The finite difference grid has to be constructed appropriately to limit numerical dispersion and to ensure accuracy, especially at locations where the solution is expected to change rapidly (Mehl et al., 2006). The structured grid of both models was refined first in the horizontal direction around the location of the ATES wells. Within a square area of 40 by 40 meters around the wells, the grid size was set to 1 m which is coherent with a minimal longitudinal dispersivity of 0.5 (Peclet number). The grid was also smoothed so that the ratio of the width of adjacent cells is not larger than 1.2. Vertically, for the model of Rijkevorsel, the two aquifer layers corresponding to the Diest Formation were further subdivided into 2 m thick layers. Below and above the Diest Formation the grid size is gradually increasing taking into account that the ratio of the horizontal and vertical cell size should not be larger than 10. The two aquifer layers of the model of the alluvial aquifer were each subdivided into layers of 1 m thickness. Above, the soil layer was subdivided into layers of 0.5 m thickness to accurately represent heat transport processes. Below, also the shale bedrock was discretized with several 1 m thick layers to account for the weathering in the upper part of the shale bedrock and to allow for a correct calculation of conduction losses in these layers (Vandenbohede et al., 2014). For both models, it was confirmed that if the grid size were further decreased, the solution would not become more accurate. For cases 1 and 2, this respectively results in a grid of 88 rows by 126 columns by 49 layers and a grid of 88 rows by 127 columns by 34 layers.

S2: Numerical methods

To solve the groundwater flow equation the preconditioned conjugate gradient (PCG) package was used. For heat transport an implicit finite-difference method for dispersion (DSP package), sinks/sources (SSM package) and reactions (RCT package) was used that applies the generalized conjugate gradient (GCG) solver. The convergence criterion of relative concentration was set to 10^{-10} as recommended by Vandenbohede et al. (2014). This is opposed to the traditional values of 10^{-5} to 10^{-6} for solute transport but is required to accurately calculate conduction and is thus of substantial importance when modelling ATES systems where (thermal) diffusion is dominant over dispersion (more dominant further from the wells). If the criterion is set too low, the heat losses by conduction are very low and the total energy efficiency of ATES is strongly overestimated.

For the model of Rijkevorsel, the total variation diminishing (TVD) method was used to solve the advection-dispersion transport equation. However, default settings led to numerical dispersion issues, particularly noticeable in model realizations with a high groundwater flow. By default, the model calculates the initial step size (dt0) based on the specified Courant number. Lowering the Courant number (PERCEL) from 1 up to 0.1 did not improve the solution. Analysis of the transport listing file (.mls) revealed that the transport steps were too large to meet the stability criteria for advection, dispersion and sink/source terms (Courant criterion). Limiting the maximum transport step size (TTSMAX) to 950 seconds proved effective. If this adjustment results in an excessive number of transport steps within a time step, it is advised to shorten the duration of the flow steps.

For the alluvial aquifer, the method of characteristics (MOC) was used instead due to persistent numerical issues encountered with the TVD method, even with TTSMAX settings of tens of seconds. This emphasizes that no single solution method is effective for all transport conditions. The lower aquifer layer has a very high conductivity attributed to the presence of clean gravel. The MOC method is known to tackle advection-dominated problems effectively underscoring its suitability for this case. However, it is worth noting that the MOC method takes a significantly longer simulation time (which we experienced was closely linked to the value of longitudinal dispersion). The solver settings were set to a maximal number of particles (MXPART) of 75000000 (obtained by trial and error) with a minimum (NPMIN) and maximum (NPMAX) number of 16 and 32 particles per finite-difference cell, respectively.

To validate the output of the model, the minimum, maximum and mean model realizations were each separately validated. They were checked in detail on the absence of numerical dispersion and on giving a realistic model response (from experience). The temperature distribution in space was visually analyzed for different stress periods. The temperature evolution with time was also analyzed for each layer of the storage aquifer separately.

S3: Justification of uncertainty ranges of the prior distribution

The lower limit of the annual storage volume corresponds to the volume of the first authorized ATES system in Liège, Wallonia (De Schepper et al., 2020). The upper limit corresponds to what is believed to be a global maximum for shallow alluvial aquifers with up to 10 m in thickness as estimated by Fossoul et al. (2011).

The soil temperature and recharge values are based on climatological data in the neighbourhood of the study area.

For case 1, the range of variation in the upper aquifer (Aqf 1) corresponds to relatively coarse sand with a loam fraction to very coarse sand while the range of the lower aquifer (Aqf 2) corresponds to very fine loam-bearing sand to relatively fine sand. The upper part of case 2 (Aqf 1) has conductivity values 1 to 2 orders of magnitude lower than the lower part which is gravely (Aqf 2).

S4: DGSA results of model realizations with constant soil temperature

The insignificance of the influence of seasonal soil temperature variations on vertical thermal energy losses/gains above the storage volumes is further supported by the fact that the DGSA of the energy exchange gives the same results when a constant temperature is considered for the top layer (Fig. 1).

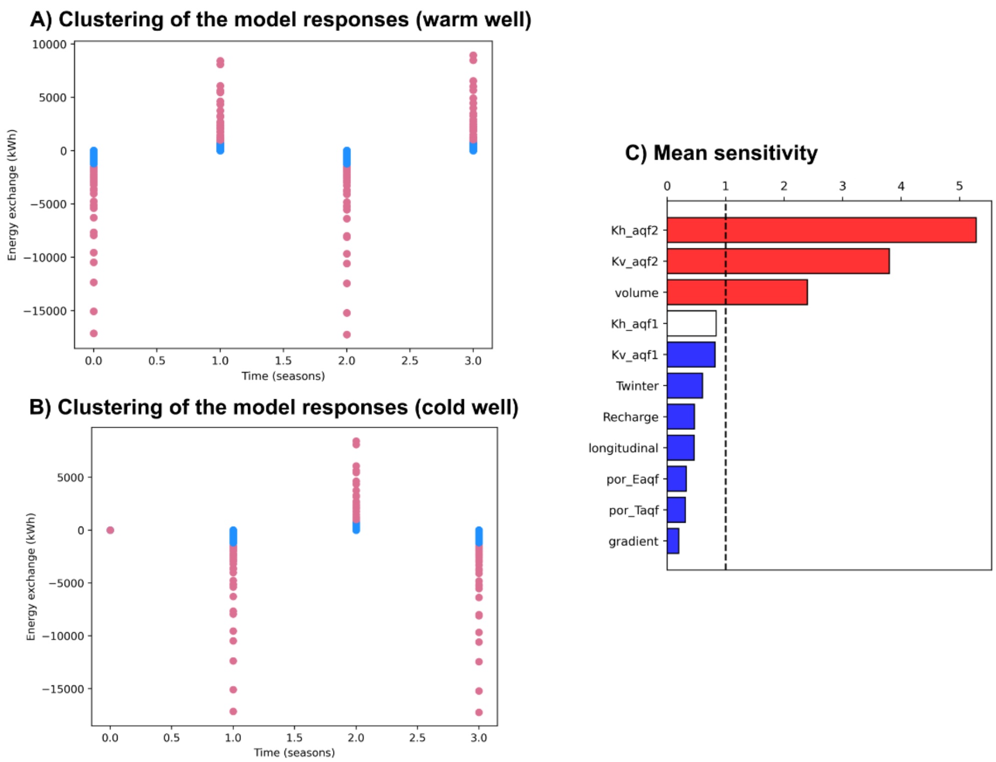

Fig. 1. *Clustering results of the energy exchange (A&B) and mean standardized sensitivity of all parameters to the vertical thermal energy exchange above the storage volume (C) when the soil temperature remains constant.*

S5: Remark on the simulation time

Case 1 and 2 were only simulated for 3 and 2 cycles respectively to limit the computational demand. This means that the dynamical equilibrium was not yet reached after the simulation time stopped. The thermal recovery efficiency of the last season was plotted against the thermal recovery efficiency of the second last season to analyse whether this choice affects the outcome (Fig.2). The scatter plot shows a small spreading which indicates that the results will be consistent also for further cycles.

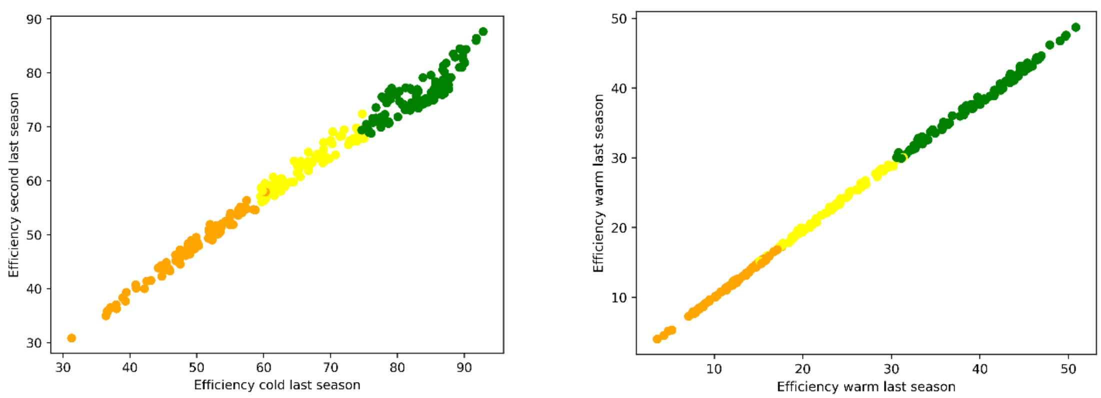

Fig. 2. *Scatter plot comparing the efficiency of the last two seasons for the cold and warm well for case 1.*

The cluster distributions of the difference in efficiency between the two last simulated seasons were also analyzed (Fig. 3). This shows that the increase in thermal recovery efficiency is the largest for the high cluster. Only in the unlikely case that the models of the medium cluster would take significantly longer to stabilize compared to the high cluster, the clustering might be different for the upcoming cycles. So we can conclude that the absolute value of the thermal recovery efficiency will change in the upcoming cycles that were not simulated but the relative cluster distribution will stay stable. These analyses validate the results of this study which are based on the interpretation of the relative efficiencies.

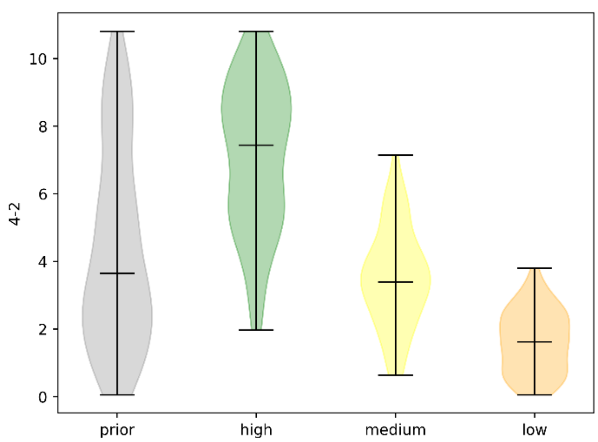

Fig. 3. *Example of distribution of the calculated difference in thermal recovery efficiency between seasons 4 and 2.*

References

De Schepper, G., Bolly, P.-Y., Vizzotto, P., Wecxsteen, H., & Robert, T. (2020). Investigations into the First Operational Aquifer Thermal Energy Storage System in Wallonia (Belgium): What Can Potentially Be Expected? *Geosciences*, *10*(1), Article 1. https://doi.org/10.3390/geosciences10010033

Fossoul, F., Orban, P., & Dassargues, A. (2011). Numerical simulation of heat transfer associated with low enthalpy geothermal pumping in an alluvial aquifer. *Geologica Belgica*. https://popups.uliege.be/1374-8505/index.php?id=3212

Mehl, S., Hill, M., & Leake, S. (2006). Comparison of local grid refinement methods for MODFLOW. *Ground Water*, *44*, 792–796. https://doi.org/10.1111/j.1745-6584.2006.00192.x

Vandenbohede, A., Louwyck, A., & Vlamynck, N. (2014). SEAWAT-Based Simulation of Axisymmetric Heat Transport. *Groundwater*, *52*(6), 908–915. https://doi.org/10.1111/gwat.12137